Extracting DNA Twist Rigidity from Experimental Supercoiling Data

Sébastien Neukirch

Institute for Mathematics B, Swiss Federal Institute of Technology, Lausanne, Switzerland
Laboratoire de Physique Statistique, Ecole Normale Supérieure, Paris, France

(Received 23 February 2004; published 5 November 2004)

We use an elastic rod model with contact to study the extension versus rotation diagrams of single supercoiled DNA molecules. We reproduce quantitatively the supercoiling response of overtwisted DNA and, using experimental data, we obtain an estimate of the effective supercoiling radius and of the twist rigidity of *B*-DNA. We find that the twist rigidity of DNA seems to vary widely with the nature and concentration of the salt buffer in which it is immersed.

DOI: 10.1103/PhysRevLett.93.198107 PACS numbers: 87.15.La, 05.45.–a, 36.20.–r, 62.20.Dc

Primarily the DNA molecule simply is the carrier of our genetic code. But in order to understand how a 2 m long string of DNA can fit into a 10 μm nucleus, one has to also consider its mechanical properties, namely, the fact that the DNA double helix is a long and thin elastic filament that can wrap around itself or other structures. These mechanical properties will in general depend on the sequence of base pairs (bp) of which the molecule is made. Nevertheless the behavior of long molecules, i.e., more than a hundred bp, is well described by a coarse-grained model known as the wormlike chain [1], where DNA is considered as a semiflexible polymer with a bending persistence length A. This is the contour length over which correlations between the orientation of two polymer segments is lost. It can be viewed as the ratio of the elastic bending rigidity K_0 to the thermal energy k_BT; hence $K_0 = Ak_BT$. The commonly accepted value is $A = 50$ nm in a physiological buffer. In the magnetic tweezer experiment [2] a single DNA molecule (of total contour length L) is anchored on a glass surface at one end, and glued to a magnetic bead at the other end, see Fig. 1. A magnet controls the bead and transmits to it a twisting moment and a pulling force F. The force is tuned via the monitored distance between the magnet and the bead and its intensity is measured using the Brownian motion of the bead. In order to input a twist constraint into the system, one gradually rotates the magnet around an axis perpendicular to the glass surface. Experiments are carried under constant force F, and the end-to-end distance Z of the DNA molecule is recorded together with the number of turns, n, made on the bead. Since no direct measurement of the twist moment is possible with magnetic tweezers, the twist persistence length C is not directly available. When no rotation is put in, the DNA molecule behaves like a semiflexible polymer, i.e., the relative extension $z = Z/L$ is a function of the temperature T, the persistence length A, and the applied pulling force F [3]:

$$z(n = 0) = 1 - \sqrt{k_BT/(4AF)}. \quad (1)$$

A refined version of this relation is used to extract A values from the experimental data [4]. Then under gradually increased rotation, the extension z decreases with the number of turns n put in and eventually the molecule starts to wrap around itself. Geometrically speaking, the DNA molecule is coiling around itself in a helical way. Since the molecule is already a double helix, we refer to this as supercoiling. Each helical wave of the superhelix is called a plectoneme. Different theoretical studies have been applied to this experiment, introducing the concepts of wormlike rod chain [5], or the torsional directed walk [6], but neglecting self-contact. Monte Carlo simulations of a model chain with hard-wall contact and an effective diameter have also been performed [7]. Plectonemic structures were considered in [8] by introducing the superhelix solution in the free energy of the chain.

Here we present an elastic model that specifically includes self-contact but leaves out thermal fluctuations. Our point is that, in the regime where plectonemes are formed, the relevant physical information is already present in our zero-temperature elastic rod model with hard-wall contact. In order to focus on supercoiling, we

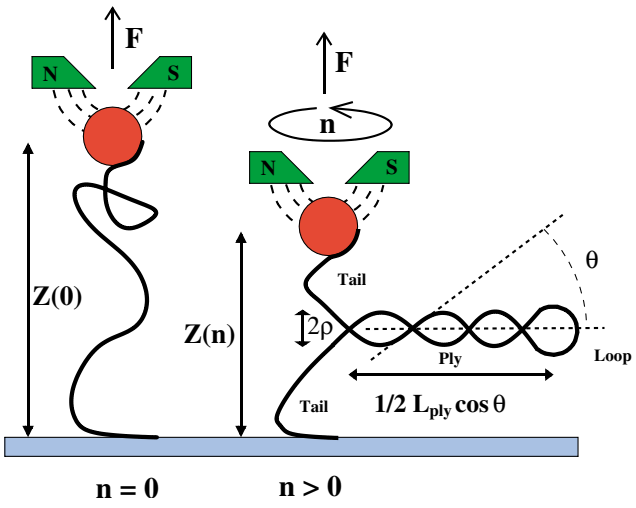

FIG. 1 (color online). The magnetic tweezer experiment.

consider the simplest elastic rod model that includes twist effects and can have 3D shapes. Following the classic terminology of the *Euler planar elastica* for twistless 2D shapes, we call the present model the *Kirchhoff ideal elastica* [9]. The elastic energy reads

$$E = \frac{1}{2}\int_0^L (K_0\kappa^2(s) + K_3\tau^2(s))ds,$$

where s is the arclength, $\kappa(s)$ the curvature of the center line, $\tau(s)$ the twist rate of the cross section around the center line (in the case of an ideal elastica τ is a constant of s), and K_0 and K_3 are the bending and twist rigidities, respectively. The Kirchhoff equilibrium equations read

$$\mathbf{F}'(s) + \mathbf{p}(s) = \mathbf{0} \tag{2}$$

$$\mathbf{M}'(s) + \mathbf{r}'(s) \times \mathbf{F}(s) = \mathbf{0} \tag{3}$$

where $\mathbf{F}(s)$ and $\mathbf{M}(s)$ are the internal force and moment, respectively. The external force per unit length $\mathbf{p}(s)$ can model electrostatic repulsion, gravity or hard-wall contact. The center line of the rod is given by $\mathbf{r}(s)$ and $\mathbf{t}(s) = \mathbf{r}'(s)$ is its tangent. In the case of an ideal elastica it can be shown [10] that

$$K_0\mathbf{t}'(s) = \mathbf{M}(s) \times \mathbf{t}(s) \tag{4}$$

$$K_0\mathbf{d_1}'(s) = (\mathbf{M}(s) - \tau(K_3 - K_0)\mathbf{t}(s)) \times \mathbf{d_1}(s) \tag{5}$$

where $\mathbf{d_1}(s)$ is a unit vector, lying in the cross section, that follows the twist of the cross section around the center line. For a DNA molecule, it is generally taken as the vector pointing toward the major groove. For the parts free of contact, we have $\mathbf{p}(s) \equiv \mathbf{0}$. In the case of self-contact there are two points along the rod, say at arclengths s_1 and s_2, where the interstrand distance $|\mathbf{r}(s_1) - \mathbf{r}(s_2)|$ is equal to twice the radius of the circular cross section (which we denote by ρ). At point s_1, we introduce a finite jump in the force vector $\mathbf{F}(s)$:

$$\mathbf{F}(s < s_1) = \mathbf{F}(s > s_1) + \delta F_{12}[\mathbf{r}(s_1) - \mathbf{r}(s_2)]/2\rho \tag{6}$$

where δF_{12} is a positive real number. The same treatment is done at point s_2, with the same δF_{12} [10,11]. This corresponds to having a Dirac function for $\mathbf{p}(s)$ in (2). In the case of continuous sections of contact, $\mathbf{p}(s)$ is a function with changing direction and intensity. In our model we only consider cases where the contact occurs either at discrete points or along straight lines. This model has already been used [12,13] and is well described in [11]. We numerically find equilibrium configurations matching the boundary conditions using classical path following techniques; first a self made algorithm relying on multiple (or parallel) shooting, then using the code AUTO [14] that discretizes the boundary value problem with a refined finite differences scheme. The different types of solutions (straight, buckled, supercoiled) are found in the following way. We fix the radius ρ and the vertical component F of the force vector $\mathbf{F}(s = 0)$ acting on the bead. We start with a straight rod with no rotation ($z = 1, n = 0$) and we twist the rod gradually. This corresponds to following the $z = 1$ line on Fig. 2 (σ is proportional to n). At point b_0, the path of straight solutions crosses the path of buckled solutions. Following this new path, configurations get more and more buckled, and eventually (at point b_1), we cross another path of solutions with one discrete contact point. At b_2, this latter path will intersect a path of configurations with two contact points. At b_3 solutions with three discrete contact points arise, and eventually, at b_4, they bifurcate to solutions including a line of contact in addition to discrete contact points. We call them *supercoiled configurations*. In a supercoiled configuration, the parts that are in continuous contact have a helical shape. We call this twin superhelix a *ply*. The ply is defined by its radius ρ and its helical angle θ (see Fig. 1). Each time we choose a different force F or radius ρ, the entire numerical continuation has to be rerun. Since we do not consider thermal fluctuations, it is no wonder that the first part (b_0 to b_2) of our numerical response curve does not correspond to what is found experimentally. On the other hand our model reproduces quite precisely the part of the response curve where the distance z decreases linearly with n, provided we identify ρ not with the crystallographic radius of the DNA molecule but with an effective supercoiling radius due to electrostatic as well as entropic repulsion. We numerically find that in the linear regime the helical angle θ does not vary with n. We fit numerical solution curves as in [15] and find that θ only depends on F, K_0, and ρ:

$$\rho^2 F = K_0\phi(\theta) \quad \text{with } \phi(\theta) = 1.658\theta^4. \tag{7}$$

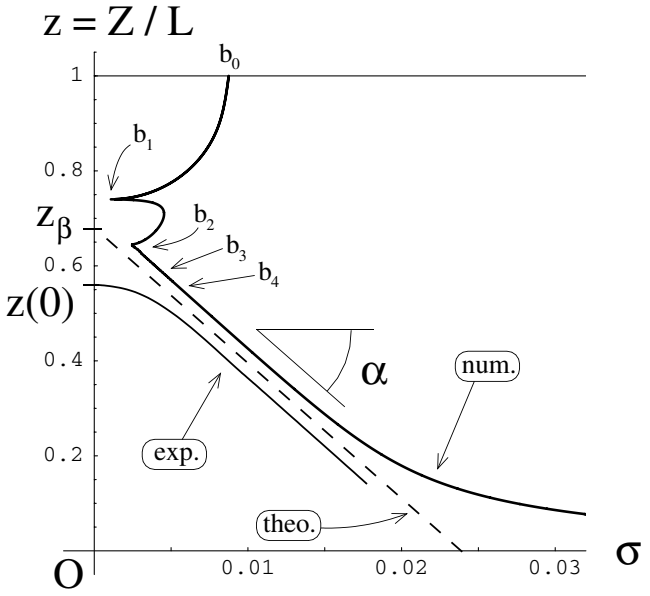

FIG. 2. Fitting the linear part of the response curve.

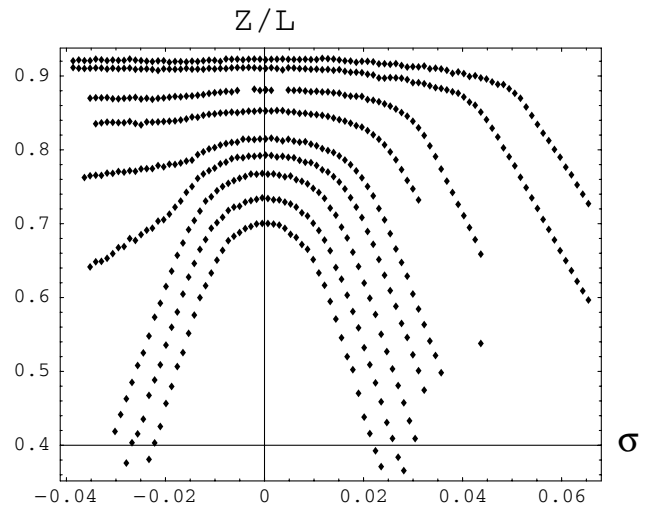

FIG. 3. Experimental response curves with a 48 kbp DNA molecule in a 10 mM phosphate buffer. The different curves correspond to experiments carried out at fixed force (from bottom to top, 0.25, 0.33, 0.44, 0.57, 0.74, 1.1, 1.31, 2.2, and 2.95 pN) [25].

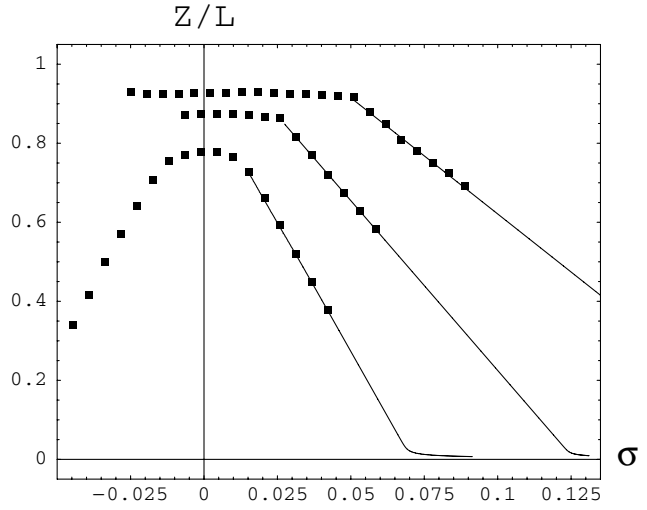

FIG. 4. Experimental data [26] taken with a 11 kbp DNA molecule in a 150 mM phosphate and 5 mM magnesium (Mg2 +) buffer. Forces are, from bottom to top, 0.45, 1.45, and 4.3 pN. The curves are numerical results of simulations of an elastic rod with contact with the values of ρ and K_3/K_0 of Table II.

This result enables us to extract the effective supercoiling radius ρ and the twist rigidity K_3 from magnetic tweezer experiments on DNA. First we note that the number of turns n applied to the magnetic bead can be interpreted as the excess link of the DNA molecule: $n = \Delta Lk$. Link is normally defined for a closed ribbon but careful use of a closure permits the introduction of the link of an open DNA molecule [16,17]. We use the Călugăreanu-White-Fuller theorem to decompose the excess link

$$(n =)\Delta Lk = \Delta Tw + Wr \tag{8}$$

where ΔLk (ΔTw) is the difference between the actual link (twist) and the intrinsic link (twist) of the double helix. The writhe Wr is the average number of crossings of the center line one sees when looking at the molecule from all possible viewpoints. Mechanical balance of the ply imposes a relation between the twist rate and the helical angle θ [11]:

$$\tau = (-\epsilon)K_0(\tan 2\theta - \sin 2\theta)/(2\rho K_3), \tag{9}$$

where $\epsilon = \pm 1$ stands for the chirality of the ply [18]. Since the twist rate is constant along the rod, we have $\Delta Tw = \tau L/(2\pi)$. Generally writhe is not additive, but using Fuller's theorem [19] with a carefully chosen reference curve we may write $\mathrm{Wr} = \mathrm{Wr}_{\mathrm{loop}} + \mathrm{Wr}_{\mathrm{tails}} + \mathrm{Wr}_{\mathrm{ply}}$ (we neglect $\mathrm{Wr}_{\mathrm{loop}}$ and $\mathrm{Wr}_{\mathrm{tails}}$). Directly computing the writhe from the double integral yields [16]

$$\mathrm{W\,r}_{\mathrm{ply}} = (-\epsilon)L_{\mathrm{ply}} \sin 2\theta/(4\pi\rho). \tag{10}$$

The total contour length L of the DNA molecule is given and we write $L_{\mathrm{ply}} = L - L_{\mathrm{loop}} - L_{\mathrm{tails}}$. We neglect L_{loop} and we set $L_{\mathrm{tails}}/Z(\sigma) = L/Z(0)$ in order to account for thermal fluctuations in the non-supercoiled region. Positive supercoiling ($n > 0$) yields a left handed ply ($\epsilon = -1$) and from (8)–(10) we have

$$\frac{\Delta Lk}{L} = \frac{\sin 2\theta}{4\pi\rho}\left[\frac{K_0}{K_3}\left(\frac{1}{\cos 2\theta} - 1\right) + 1 - \frac{Z}{Z(0)}\right]. \tag{11}$$

The intrinsic twist of the DNA double helix is $Lk_0 = L/H$, where $H = 3.57$ nm is its pitch. We introduce the supercoiling ratio $\sigma = \Delta Lk/Lk_0 = nH/L$ and invert Eq. (11) to arrive at an approximation of the linear part of the response curve in the (σ, z) plane:

$$\frac{z}{z(0)} = 1 + \frac{K_0}{K_3}\left(\frac{1}{\cos 2\theta} - 1\right) - \frac{4\pi\rho}{H \sin 2\theta}\,\sigma. \tag{12}$$

Given that experiments are carried at given (fixed) F and that K_0 is obtained from (1) with $K_0 = Ak_BT$, to extract

TABLE I. Results for the 48 kbp DNA molecule in a 10 mM phosphate buffer. Fitting data at $\sigma = 0$, as in [4], yields $K_0 = (51 \pm 2)$ nm k_BT.

F (pN)	θ (rad)	ρ (nm)	K_3/K_0	K_3/k_BT (nm)
0.25	0.427	6.85	1.88	97
0.33	0.449	6.60	1.87	96
0.44	0.467	6.17	1.92	99
0.57	0.469	5.47	1.84	95
0.74	0.504	5.55	2.01	103
1.1	0.488	4.26	1.86	95
1.31	0.471	3.64	1.58	81
2.2	0.503	3.21	1.65	85
2.95	0.507	2.81	1.62	83

TABLE II. Results for the 11 kbp DNA molecule in a 150 mM phosphate and 5 mM magnesium ($Mg2+$) buffer. Fitting data at $\sigma = 0$, as in [4], yields $K_0 = (57 \pm 3)$ nm k_BT.

F (pN)	θ (rad)	ρ (nm)	K_3/K_0	K_3/k_BT (nm)
0.45	0.307	2.79	1.09	62.5
1.45	0.319	1.67	1.00	57.3
4.3	0.348	1.15	0.99	56.5

information from the experimental data such as in Fig. 3 or Fig. 4, we need, for each curve in the (σ, z) plane: (i) the relative extension at $\sigma = 0$, which we denote by $z(0)$, (ii) the slope, which we denote by α, (iii) and the ordinate at the origin, which we denote by z_β, of the straight line fitting the linear part of the response curve. Using (7) and (12) we obtain an equation for θ:

$$\alpha H \sin 2\theta = -4\pi z(0)\sqrt{K_0 \phi(\theta)/F}. \tag{13}$$

With θ known, we obtain the effective supercoiling radius from (7) and the effective stiffness ratio from (12):

$$K_3/K_0 = (1 - 1/\cos 2\theta)/(1 - z_\beta/z(0)). \tag{14}$$

In order to check the consistency of our method, we have performed numerical simulations of supercoiled configurations using ρ and K_3/K_0 values from Table II. The resulting curves (each one starting at its b_4 point) are plotted in Fig. 4. From the results shown in Table I and II, we see that the effective supercoiling radius decreases with the intensity of the pulling force, and with the strength of the salt buffer and can go down to values barely larger than the DNA crystallographic radius, supporting the tight supercoiling hypothesis [20]. Present values are fairly smaller than values coming from analysis of equilibrium distributions of supercoiled plasmids [21]. Our values of K_3 can be compared to the results of [22] where another microtechnique was used and a value of $K_3 \simeq 100$ nm k_BT (in a 100 mM NaCl + 40 mM Tris-HCl buffer) was found. Previous measurements of K_3 based on different biochemical techniques (e.g., fluorescence depolarization [23]) yield values ranging from 50 to 100 nm k_BT [24]. Also Monte Carlo and other statistical physics methods applied to the data in [2] yield K_3 values from 75 to 120 nm k_BT (see [5,22] for detailed discussions). The present result seems to indicate that the divalent magnesium ions have an important effect on the twist rigidity of DNA (or at least an effect clearly different from that of monovalent ions).

It is a pleasure to thank G. Charvin and V. Croquette for supplying the experimental data, and J. H. Maddocks and D. Bensimon for discussions.

[1] O. Kratky and G. Porod, Recl. Trav. Chim. **68**, 1106 (1949).
[2] T. R. Strick, J.-F. Allemand, D. Bensimon, A. Bensimon, and V. Croquette, Science **271**, 1835 (1996).
[3] J. F. Marko and E. D. Siggia, Phys. Rev. E **52**, 2912 (1995).
[4] C. Bouchiat, M. D. Wang, J.-F. Allemand, T. Strick, S. M. Block, and V. Croquette, Biophys. J. **76**, 409 (1999).
[5] C. Bouchiat and M. Mézard, Eur. Phys. J. E **2**, 377 (2000).
[6] J. D. Moroz and P. Nelson, Proc. Natl. Acad. Sci. U.S.A. **94**, 14 418 (1997).
[7] A. V. Vologodskii and J. F. Marko, Biophys. J. **73**, 123 (1997).
[8] J. F. Marko, Phys. Rev. E **55**, 1758 (1997).
[9] S. Neukirch and M. E. Henderson, J. Elast. **68**, 95 (2002).
[10] G. H. M. van der Heijden, S. Neukirch, V. G. A. Goss, and J. M. T. Thompson, Int. J. Mech. Sci. **45**, 161 (2003).
[11] B. D. Coleman and D. Swigon, J. Elast. **60**, 173 (2000).
[12] D. M. Stump, W. B. Fraser, and K. E. Gates, Proc. R. Soc. London A **454**, 2123 (1998).
[13] Z. Gáspár and R. Németh, in Proceedings of the 2nd European Conference on Computational Mechanics, Poland, 2001 available on CD.
[14] E. Doedel, H. B. Keller, and J. P. Kernevez, Int. J. Bifurcation Chaos Appl. Sci. Eng. **1**, 493 (1991).
[15] D. M. Stump and W. B. Fraser, Proc. R. Soc. London A **456**, 455 (2000).
[16] E. L. Starostin, physics/0212095.
[17] V. Rossetto and A. C. Maggs, J. Chem. Phys. **118**, 9864 (2003).
[18] S. Neukirch and G. van der Heijden, J. Elast. **69**, 41 (2002).
[19] J. Aldinger, I. Klapper, and M. Tabor, Journal of Knot Theory and its Ramifications **4**, 343 (1995).
[20] J. Bednar, P. Furrer, A. Stasiak, J. Dubochet, E. H. Egelman, and A. D. Bates, J. Mol. Biol. **235**, 825 (1994).
[21] V. V. Rybenkov, A. V. Vologodskii, and N. R. Cozzarelli, Nucleic Acids Res. **25**, 1412 (1997).
[22] Z. Bryant, M. D. Stone, J. Gore, S. B. Smith, N. R. Cozzarelli, and C. Bustamante, Nature (London) **424**, 338 (2003).
[23] P. Heath, J. B. Clendenning, B. S. Fujimoto, and J. M. Schurr, J. Mol. Biol. **260**, 718 (1996).
[24] P. J. Hagerman, Annu. Rev. Biophys. Biophys. Chem. **17**, 265 (1988).
[25] S. Komolikis (unpublished).
[26] G. Charvin (unpublished).